ACTUATORS

Vital signal sensing and manipulation of a microscale organ with a multifunctional soft gripper

Yeonwook Roh[1†], Minho Kim[1†], Sang Min Won[2†], Daseul Lim[1], Insic Hong[1], Seunggon Lee[1], Taewi Kim[1], Changhwan Kim[1], Doohoe Lee[1], Sunghoon Im[1], Gunhee Lee[3], Dongjin Kim[1], Dongwook Shin[1], Dohyeon Gong[1], Baekgyeom Kim[1], Seongyeon Kim[1], Sungyeong Kim[1], Hyun Kuk Kim[4], Bon-Kwon Koo[5], Sungchul Seo[6], Je-Sung Koh[1]*, Daeshik Kang[1]*, Seungyong Han[1]*

Soft grippers that incorporate functional materials are important in the development of mechanically compliant and multifunctional interfaces for both sensing and stimulating soft objects and organisms. In particular, the capability for firm and delicate grasping of soft cells and organs without mechanical damage is essential to identify the condition of and monitor meaningful biosignals from objects. Here, we report a millimeter-scale soft gripper based on a shape memory polymer that enables manipulating a heavy object (payload-to-weight ratio up to 6400) and grasping organisms at the micro/milliscale. The silver nanowires and crack-based strain sensor embedded in this soft gripper enable simultaneous measurement of the temperature and pressure on grasped objects and offer temperature and mechanical stimuli for the grasped object. We validate our miniaturized soft gripper by demonstrating that it can grasp a snail egg while simultaneously applying a moderate temperature stimulation to induce hatching process and monitor the heart rate of a newborn snail. The results present the potential for widespread utility of soft grippers in the area of biomedical engineering, especially in the development of conditional or closed-loop interfacing with microscale biotissues and organisms.

INTRODUCTION

Achieving gentle touch with soft grippers is an important topic in human-robot interaction (*1*, *2*). The recent integration of soft, flexible, and compliant materials in soft grippers enables conformal contact and delicate handling of living organisms in a nondestructive manner. Many of these soft grippers take inspiration from nature, typically human fingers (*3*–*6*), which provide the mechanical morphology and rigidity required for artificial grippers. Furthermore, the additional integration of electrical functionality enables the mimicking of skin-like perception, similar to cutaneous sensory receptors in human fingers that detect stimuli (e.g., pressure, strain, and temperature) from the physical environment (*7*, *8*). Experimental demonstrations of these artificial grippers with sensing capabilities and soft mechanical properties illustrate their potential use in drug delivery (*9*), noninvasive biopsy (*10*), and delicate manipulation and shape detection of objects (*11*, *12*). However, devices in these soft platforms still lack bidirectional sensing and stimulating interactions with microscale and complex-shaped soft objects, partly because of the limited material selection and/or actuation methodologies (*13*). This suggest that a device that fully mimics and/or reinforces the functions of grippers in nature (e.g., human fingers) requires not only soft and robust mechanical properties but also multiple functionalities, both in sensing and stimulating objects (*14*).

Another bottleneck of soft grippers has been the limited force density (e.g., payload capacity) due to the inherent softness of the material. Here, the range of the variable stiffness of materials represents a key feature determining the force density. Research in this area aims to overcome this limitation through the use of various materials or structures such as variable stiffness dielectric elastomers (e.g., chucking electrodes) (*15*), low–melting point alloys (e.g., embedded in silicon) (*16*), polymer paper (e.g., polyester) (*17*), shape memory alloys (*18*), vacuum-sealed packages (e.g., granular jamming materials) (*19*), and pneumatic systems (e.g., octopus arms) (*20*). The range of controllable stiffness realized through these materials, however, is very narrow, so the maximum demonstrated payload-to-weight ratio has been 17 with a low–melting point alloy (*15*, *16*). The reported polymer paper with variable stiffness has a high lifting ratio, but this material has an actuation temperature of 90°C (*17*). Thus, applying it to living organisms is difficult. Other approaches using the design of a structure-controlled variable stiffness present some promise but only with relatively large and bulky objects (*18*–*20*).

Here, we present a miniaturized multifunctional and five finger-shaped soft gripper that can interact with a living organism (Movie 1). The programmable stiffness control achieved through embedded silver nanowires (Ag NWs) enables grasping of soft organisms in a low stiffness state (Young's modulus of 2 MPa) and manipulation of a heavy object (payload-to-weight ratio up to 6400) in the high stiffness state (Young's modulus of 1.4 GPa). The laser-patterned Ag NWs that allow mechanical control of each finger also enable temperature monitoring and thermal stimulation. The additional highly sensitive crack-based strain sensor incorporated with the soft gripper offers high sensitivity for the detection of mechanical vibration and strain. A key feature is the capability for bidirectional interaction with both light and heavy organisms through electrical interfaces with each of the five fingers. We validate our miniaturized soft gripper by

[1]Department of Mechanical Engineering, Ajou University, Multiscale Bio-inspired Technology Lab, Suwon 16499, Republic of Korea. [2]Department of Electrical and Computer Engineering, Sungkyunkwan University, Suwon 16419, Republic of Korea. [3]Department of Environment Machinery, Korea Institute of Machinery and Materials, Daejeon 34103, Republic of Korea. [4]Department of Internal Medicine and Cardiovascular Center, Chosun University Hospital, University of Chosun College of Medicine, Gwangju 61453, Republic of Korea. [5]Department of Internal Medicine and Cardiovascular Center, Seoul National University Hospital, Seoul 03080, Republic of Korea. [6]Department of Environmental Health and Safety, EulJi University, Seoul 11759, Republic of Korea.
*Corresponding author. Email: sy84han@ajou.ac.kr (S.H.); dskang@ajou.ac.kr (D.K.); jskoh@ajou.ac.kr (J.-S.K.)
†These authors contributed equally to this work.

Movie 1. Overview of the soft gripper for vital signal sensing and manipulation of a microscale organ. A miniaturized gripper composed of a nanowire-based heater and crack-based strain sensor enables mechanically soft and multifunctional interaction with an organism. A demonstration of the soft gripper delivering moderate temperature and monitoring heart rate of a newborn snail is reported.

demonstrating that it can grasp a snail egg, apply moderate temperature stimulation to induce hatching process, and monitor the heart rate of a newborn snail. The technology presented in this article may have potential use in closed-loop interfacing in the areas of biology, robotics, biotechnology, and biomedical applications.

RESULTS

Materials, fabrication procedures, and design

The miniaturized interactive soft gripper takes inspiration from the natural human hand shape, where the independent movement and fixation of individual fingers allow grasping, manipulation, and interaction with the environment (Fig. 1A). To achieve key mechanical and interactive properties of human hands, the system uses a shape memory polymer (SMP) that provides variable stiffness for soft and robust mechanics, a Norland optical adhesive (NOA) that induces finger-like movement, a heater that exploits Ag NWs for both temperature sensing by the gripper and thermal actuation to induce its movement, and a highly sensitive crack-based strain sensor (gauge factor, ~20,000) (*21*) that allows simultaneous measurement of the mechanical deformation and condition of grabbed organisms. Materials and Methods and fig. S1 illustrate the fabrication processes, beginning with SMP film preparation (thickness, ~400 μm) from pellet structures. Laser cutting of such a film in a deterministic direction can yield a hand-like gripper shape (angles of 15°, 30°, 45°, 60°, 75°, and 90°; fig. S2). Transfer printing of Ag NWs (thickness of ~3 μm) and subsequent coating of the NOA (thickness of ~100 μm) on top of the SMP and Ag NWs then finalize the simple soft gripper structure capable of moving without a complex motor and/or rigid joints. The additional cracked-based mechanical sensor exploits a chromium (Cr) layer (thickness of 50 nm) and a gold (Au) layer (thickness of 20 nm) on a polyimide (PI) film and is attached under the SMP. Figure S3 shows scanning electron microscopy (SEM) images of the cross section and embedded Ag NWs.

Figures 1 (B to D) presents the lightweight (25 mg) miniaturized (each finger has a width of 780 μm and a length of 6.3 mm; fig. S4) soft gripper that enables control of each finger in a programmable manner (fig. S5 and movie S1). This independent and controllable movement of each finger is a distinguishable characteristic of this soft gripper, allowing selective gripping and interaction with objects regardless of the size or shape. For example, the gripper can stably grip and lift metal washers with different diameters [3.2, 5.2, and 6.2 mm from left to right in Fig. 1 (E to G)] using a different number of fingers. Furthermore, the overall size of the gripper is suitable for gripping objects in an unexplored narrow area, as shown in fig. S6, where the gripper extracts a foreign object (polystyrene, size of 2.5 mm) from a vessel with a diameter of 3 mm.

Theoretical analysis of the movement mechanism

Joule heating through the Ag NW heaters yields a thermally induced strain mismatch between the SMP (active layer) and NOA (passive layer), with consequent mechanical bending of individual fingers as unimorph actuators (Fig. 2A) (*22*, *23*). The mechanism exploits the tensile and compressive stress induced in the passive layer and prestrained active layer, respectively, because of the difference in their moduli (NOA, ~138 MPa; SMP, ~2 MPa) as the temperature actuation occurs. Figure 2B presents the finite element analysis (FEA) results of the deformed shape of the soft gripper during the heating process, showing that the simulation results are in good agreement with the experimental results. Before actuation, at an ambient temperature of 23°C, the SMP has a stiffness of 1.4 GPa. The heat on the gripper changes the SMP stiffness to 200 MPa at 35°C. At the same time, the SMP contracts, and actuation begins. The continuous temperature rise of the gripper (~43°C) further induces a lower stiffness of the SMP, from 200 to 2 MPa, and accelerates the bending motion. Further information on FEA can be found in section 1 of Supplementary Text.

The result is a bending stress with rolling toward the active layer. Figure 2 (C and D) and fig. S7 show an infrared (IR) image and the associated temperature change of the five fingers upon applying an electrical current to each heater. The initial resistance of 190 ohms and wattage of 0.04 J/s enabled the glass transition temperature (35°C) to be reached within about 2 to 3 s at an applied voltage of 3 V. The heat on individual fingers did not affect the temperature change of adjacent fingers, yielding folding of individual fingers at a temperature above 43°C (Fig. 2, E and F). For example, the fifth finger in the figure reached the transition temperature at 2 s and the fully folded shape at 2.4 s with an applied voltage of 7.5 V. The actuation speed of the gripper can be accelerated by applying a higher voltage; for example, a 9.5-V voltage was able to actuate and initiate the folding motion within 1 s (fig. S8A). A further increase in the voltage on the Ag NW heater above 9.5 V, however, disconnected the heater, probably because of local concentration of thermal energy and consequent electrical disconnection of the Ag NWs (fig. S8, B and C).

Mechanical properties and characterization

The large variable stiffness range allows delicate handling of soft objects during the grasping motion and robust manipulation of heavy and/or complex-shaped objects during the lifting motion. Figure 3A shows the strain-stress curve of the gripper in different modulus states. The experiments followed the ASTM (American Society for Testing and Materials) D882 standard. Under ambient conditions (~23°C), the SMP layer remains in a glass region with a modulus of ~1.4 GPa. The temperature of actuation (~43°C) reduces this modulus to ~2 MPa, causing soft and rubbery-like mechanical properties. The bending amount after thermal actuation of the gripper depends

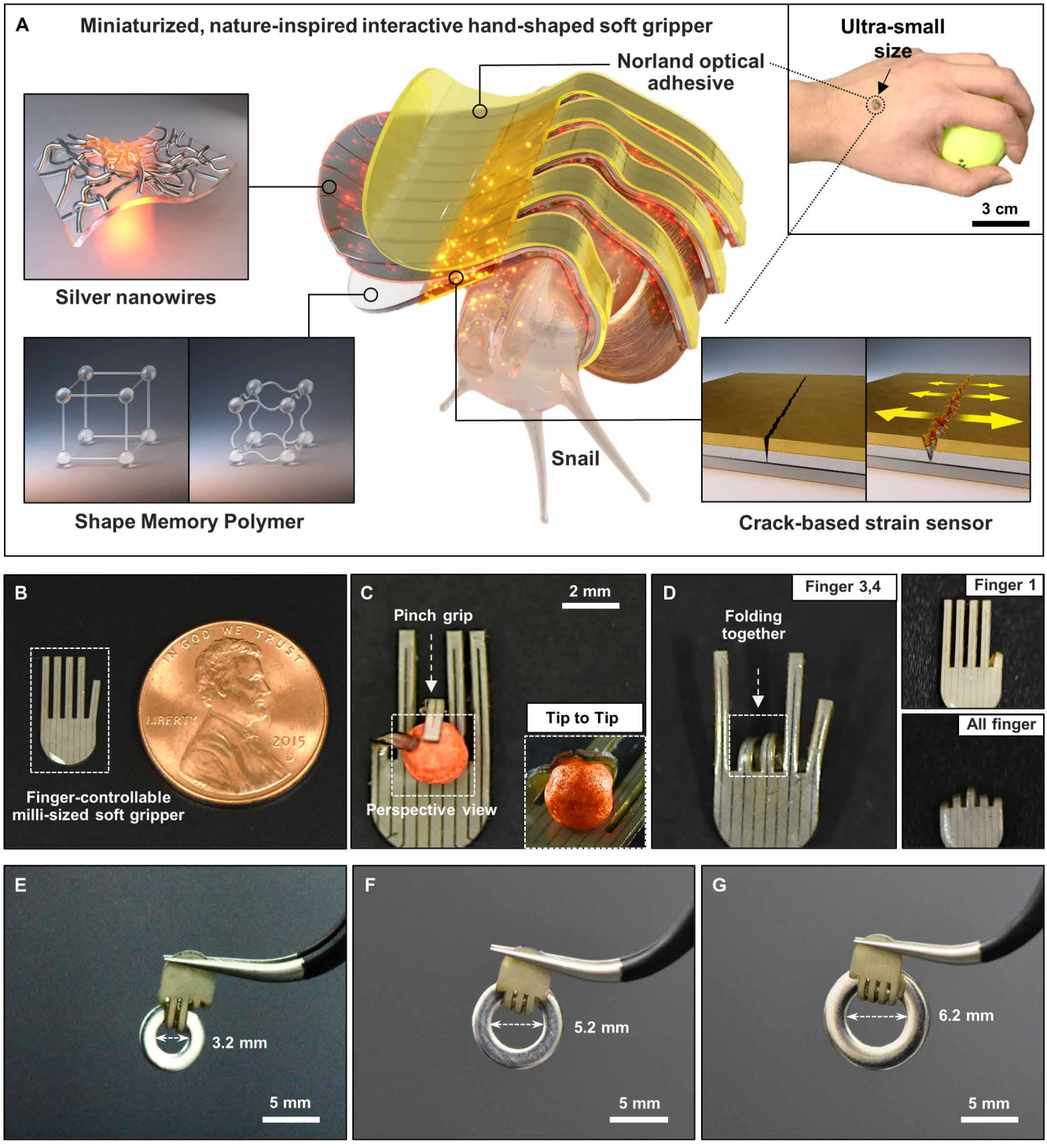

Fig. 1. Schematic illustrations and images of a miniaturized hand-shaped soft gripper. (**A**) Schematic illustration of the milliscale soft gripper with variable stiffness for measuring biosignals of a living organism. (**B** to **D**) Photographs of the milliscale soft gripper, tip-to-tip gripping using the thumb and middle finger, and selective folding of digits for various finger positions. (**E** to **G**) The soft gripper selectively grips the object using fingers depending on the object size.

on the prestrain (~200%) of the SMP before Ag NW and NOA integration and the thickness ratio between the NOA and SMP layers. A large value of the former leads to an increase in the recovery force, with a consequent decrease in the bending curvature (Fig. 3B). The latter determines the thermally induced mechanical strain mismatch between the NOA and SMP such that a decrease in the NOA thickness leads to a decrease in the bending curvature (Fig. 3C) (*24*).

Tests of the payload capacity of the gripper show the capability for lifting and manipulating objects 1200 times heavier (30 g) than the gripper weight (0.0254 g) for a time period of more than 3 min

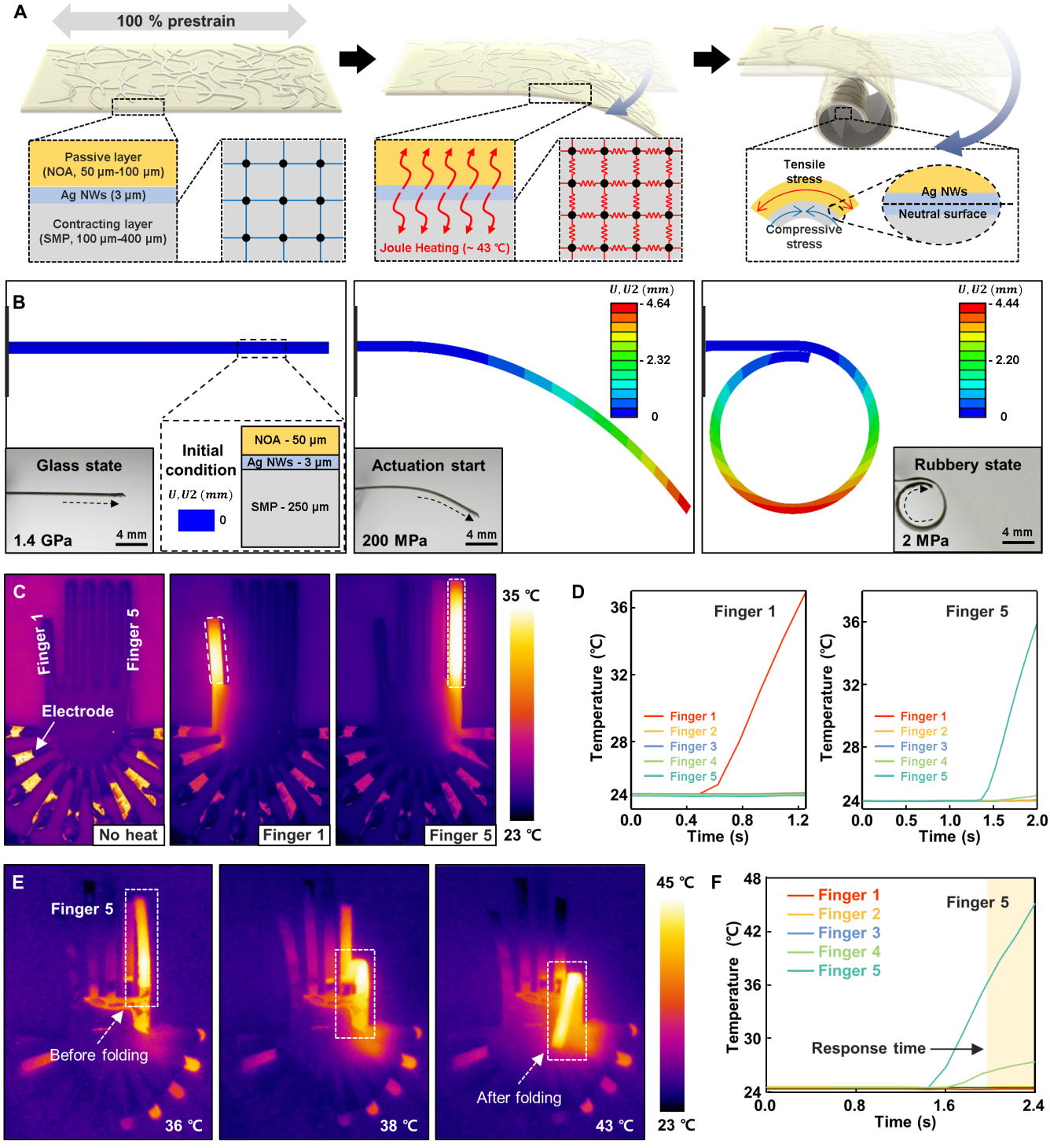

Fig. 2. Actuation mechanism of the soft gripper. (**A**) Schematic illustration of finger folding due to a mechanical strain mismatch during Joule heating. (**B**) FEA models of the bending motion of the soft gripper. (**C**) IR camera images of the soft gripper viewed from the top before and after a voltage was applied. (**D**) Temperature profiles of finger 1 and finger 5 under Joule heating to the glass transition temperature. (**E**) IR camera images of the folding sequence for finger 5 in the top view. (**F**) Temperature and actuation velocity profiles for actuated finger 5 and the other fingers.

(Fig. 3D). The gripper could withstand forces of up to ~0.07 N (or 7.1 g, 280 times), 1.05 N (or 107 g, 4213 times), and 1.6 N (or 163 g, 6400 times) for one, three, and five fingers, respectively, assessed through a tensile testing machine (3342 UTM, Instron Co.) (Fig. 3E and fig. S9). These results indicate the highest payload capacity among soft grippers presented to date (fig. S10 and table S1).

The gripper demonstrated conformal grasping and manipulation of both a rigid cap (diameter of ~12 mm) (Fig. 3F) and soft

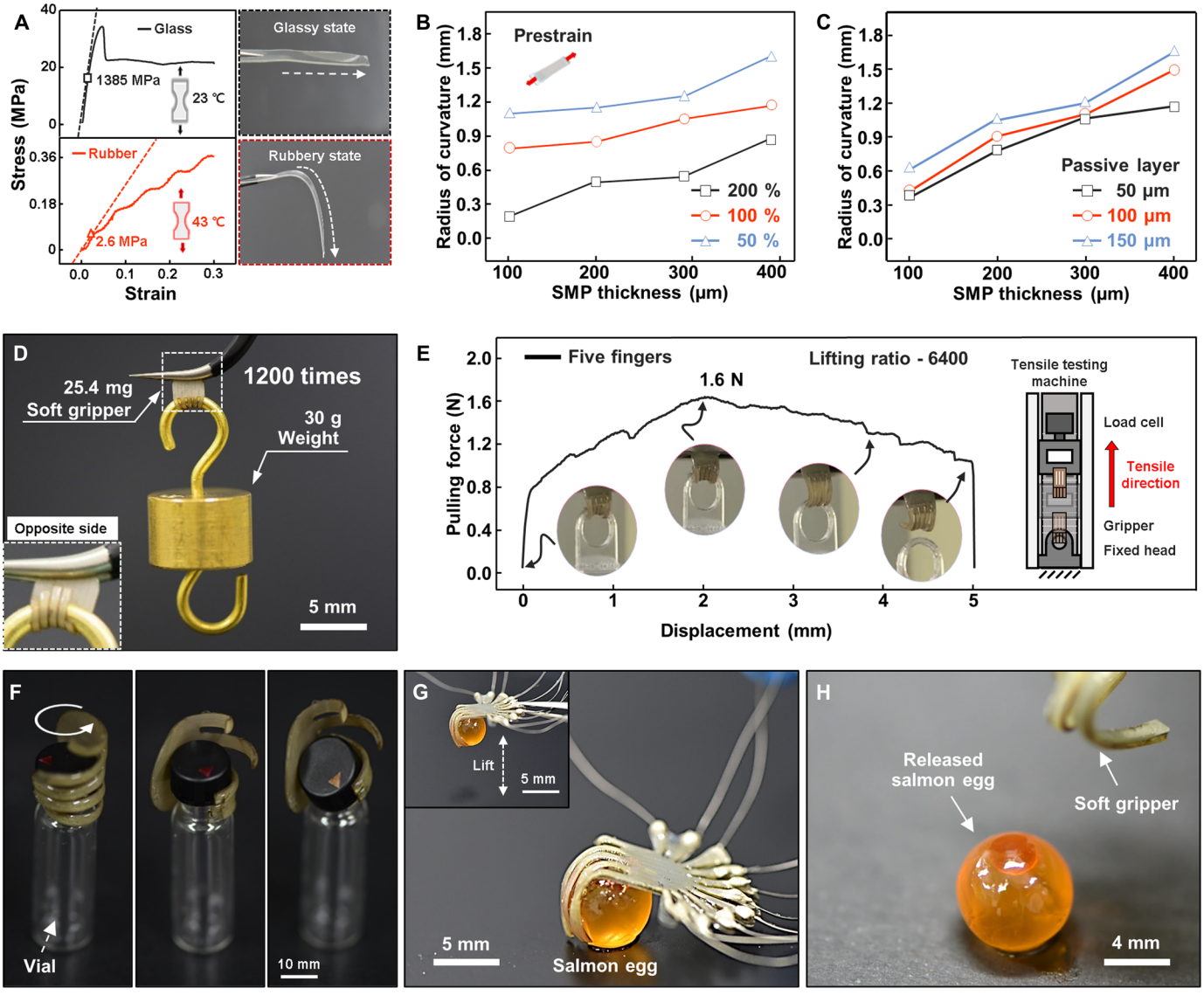

Fig. 3. Characterization and performance of the soft gripper using variable stiffness. (**A**) Young's modulus and images of the SMP in its glassy and rubbery states. (**B**) Radius of the finger curvature depending on the SMP thickness and prestrain of the SMP (passive layer thickness, 50 μm). (**C**) Radius of the finger curvature depending on the thicknesses of the SMP and passive layer (prestrain of the SMP of 100%). (**D**) Front and rear views of the soft gripper lifting a balance weight (30 g). (**E**) Measurement of the pulling force of the five fingers. (**F**) Opening a vial using the soft gripper, maintaining conformal contact in the variable stiffness mode. (**G**) Soft gripper gripping and lifting a salmon egg. (**H**) Soft gripper releasing the salmon egg without damage.

salmon eggs (diameter of 6 mm) (Fig. 3, G and H), well known for fragility, through the thermal actuation. The conformal contact and hard stiffness in the former case allowed tight holding and high bending stiffness for five fingers, respectively, and consequent opening of the bottle with a tight lid. The actuation temperature (~43°C) for gripping objects is another key characteristic that enables utilization with a living organism, such as in the latter case, where the threshold temperature for short time intervals (~3 s) without thermal damage is ~43°C (*25*).

Functional gripper with sensing and stimulation capabilities

An important modality for clear interpretation of the behavior and other physical changes of gripped living organs and other objects is to monitor physiological signals. Figure 4A shows a photograph and a schematic illustration of the crack-based strain sensor (inset image) integrated on the gripper, where the Ag NW at each finger can monitor the temperature and stimulate thermal energy, whereas the resistive crack-based strain sensor on the back of the gripper can measure any mechanical deformation that the soft gripper is subjected to.

Mechanical deformation (i.e., pressure, stretching, and bending) of the gripper induces a change in the crack structure with a consequent change in the resistance of the strain sensor on the back of the gripper. The key material is the gold layer with zigzag cracks that disconnect and reconnect during stretching and shrinking, respectively, and behave as a highly sensitive strain gauge on the soft gripper (Fig. 4B). Figure S11 presents the sound signal produced by a tuning fork through crack structure changes. The measured sound signal was calculated to be 0.02 Pa, and the response time was 50 ms

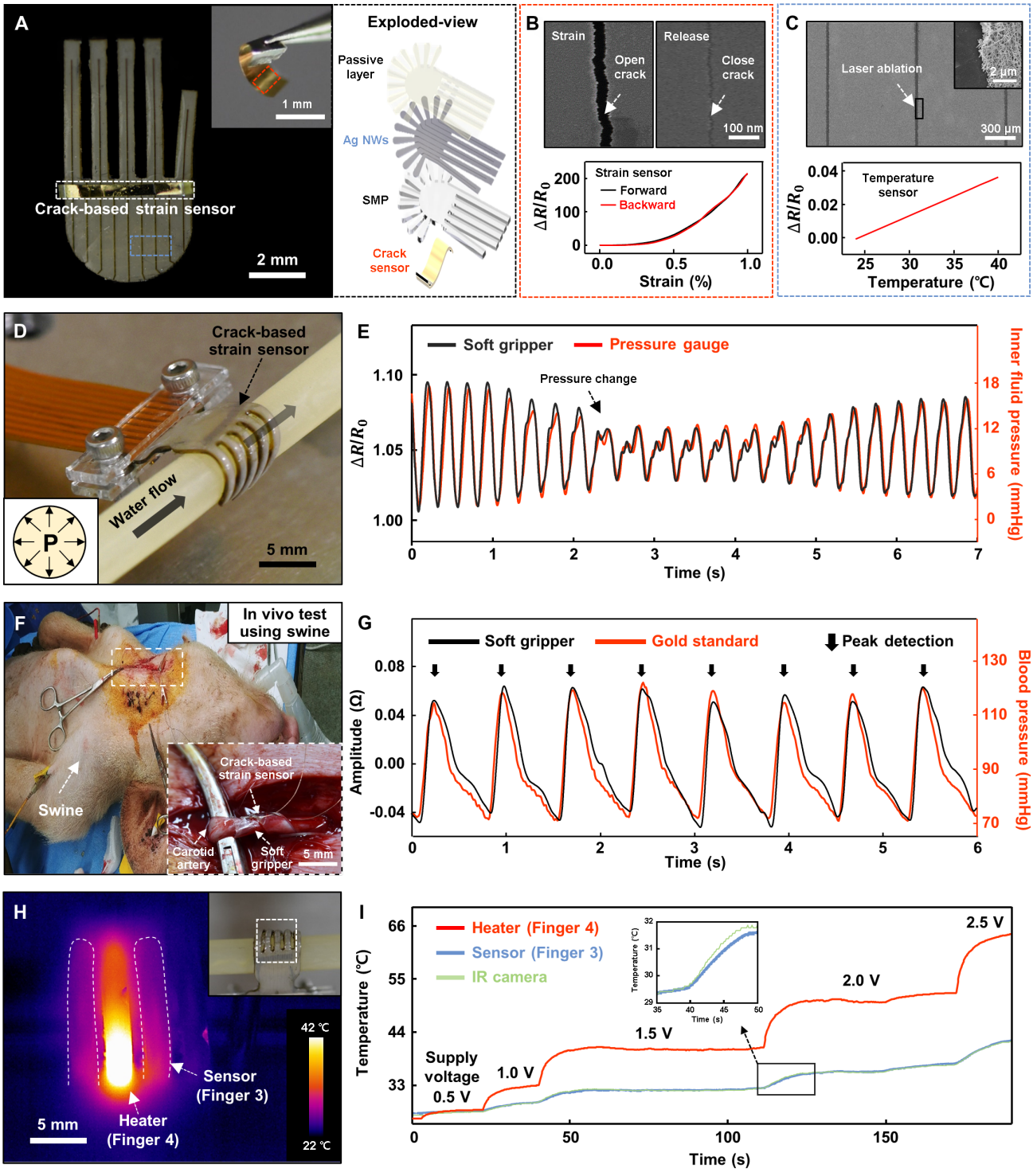

Fig. 4. Mechanical signal monitoring and stimulation with the soft gripper incorporated with a crack-based strain sensor and Ag NWs. (**A**) Photographic and exploded-view schematic images of the soft gripper supplying heat to a grasped object while simultaneously measuring the temperature and pressure of the object. (**B**) SEM image and hysteresis graph of the crack-based strain sensor. (**C**) SEM image of Ag NW ablation and sensitivity of Ag NWs. (**D**) Soft gripper holding an artificial blood vessel through which water is pumped to simulate an artery system. (**E**) IFP of the artificial artery system measured via the soft gripper (black line) and a commercial pressure gauge (red line). (**F**) The soft gripper holding a carotid artery of a swine. (**G**) Carotid artery pressures monitored with the soft gripper and a 4-Fr sheath. (**H**) IR camera image of the soft gripper supplying heat to a grasped object while simultaneously measuring the temperature of the object (heat provided via finger 4 and temperature measured via finger 3). (**I**) Comparison of the temperatures of the grasped object as measured via the soft gripper (blue line) and the IR camera (green line).

(fig. S12, A and B). These results are comparable with those of other highly sensitive strain gauges and human hands in terms of performance (table S2). Further details of the crack-based strain sensor fabrication process, performance, and evaluation process are provided in the Supplementary Materials (sections 2 and 3 of Supplementary Text and fig. S12, C and E).

The temperature-sensing mechanism exploits the thermal resistivity coefficient (0.37 ohm/°C) of Ag NWs (Fig. 4C), comparable with that of nanomaterials used in epidermal temperature sensors (*26*). The calibration procedure for recording temperature at a sampling rate of 25 Hz involves matching the data with those collected from an IR camera (sensitivity of 0.05°C) without a substantial difference (less than 1°C) for each sensor on the five fingers. The detailed calibration process for the temperature sensor is outlined in the Supplementary Materials (section 4 of Supplementary Text and fig. S13, A and B) Here, the sensing capability at a separate fingertip enables detailed mapping of the temperature throughout the gripper fingers. For example, the temperatures at the index and little fingers in fig. S13 (C and D) show a ~3°C difference, whereas light-emitting diodes, with a temperature of ~34°C at 5 V, are held adjacent to the index finger. Temperature comparisons between the other fingers under the same conditions are shown in fig. S13 (E to G). Joule heating is used to achieved thermal stimulation, where applied voltage and resistance of Ag NWs determine the thermal power (fig. S14A). Here, different composite percentiles of Ag NWs embedded in the soft gripper decide the unique resistance value (fig. S14B). The temperature increments in fig. S14C show the temperature change of about 1°C as the supplied voltage increases by 0.1 V. Figure S14D displays the Joule heating cycling test, repeated 10 times. The gripper maintains the following temperatures in each cycle for 180 s: 1.0 V, 28°C; 1.5 V, 33°C; and 2.0 V, 43°C. The demonstration indicates the feasibility of temperature control through supplying voltage and composite percentiles of Ag NWs and with durability in various heating conditions (fig. S14E).

The soft gripper integrated with the crack-based strain sensor was used to monitor the mechanical movements of a salmon egg in response to touch (fig. S15). We also simulated a human artery system, as shown in the illustrated setup (fig. S16A), to test the potential for using the soft gripper to monitor a human pulse in a blood vessel (artificial blood vessel, ~1.8 MPa; human blood vessel, ~0.5 to 1 MPa) (*27*). The artificial human artery system could produce pulse-like waves and pressure changes in the artificial blood vessel. (The details of the artificial human artery system setup and performance are given in section 5 of Supplementary Text and fig. S16.) To measure accurate signals from the artery system, the soft gripper has to make conformal contact with the artificial blood vessel and remain fixed (Fig. 4D) (*28*). The inner fluid pressure (IFP) of the artificial human artery system could be measured through the crack-based strain sensor (Fig. 4E and movie S2). These measured values of the IFP were similar to the IFP measured by a commercial pressure gauge (fig. S16D). To further test the application potential of our soft gripper in a biomedical device, we designed an in vivo test using a swine. The soft gripper, combined with the crack-based strain sensor, was used to measure the pig's carotid pulse waves and blood pressure. We compared our measurements with those obtained using a 4-french (Fr) sheath, which is considered the gold standard for blood pressure measurement, as a reference sensor. In our experiments, the soft gripper made soft conformal contact with the swine's carotid and firmly fixed onto it to measure its blood pressure (Fig. 4F). As our measurement results show, no measurable differences occur between the peaks detected with the soft gripper and the 4-Fr sheath when monitoring the IFP in the pig carotid (Fig. 4G). Further details of the in vivo test can be found in the Supplementary Materials (section 6 of Supplementary Text).

Figure 4H presents both the stimulation and sensing capabilities by detecting the temperature while applying thermal energy to a gripped object. The results from the sensing finger match the data from an IR camera without any noticeable difference, as shown in Fig. 4I, revealing similar temperature profiles between the IR camera and temperature sensor of the soft gripper. Although the bending motion of the soft gripper induces tensile stress on the inner electrode to grip an object, the resistance change induced by the temperature can be monitored when the neutral axis is close to the Ag NWs embedded between the SMP and passive layer, as shown in fig. S18A (*29*). The FEA and theoretical and experimental results (resistance change of 1%) demonstrate a neutral axis shift from the SMP to Ag NWs, resulting from the stiffness change of the SMP during the bending motion (diameter of 1.5 mm). Detailed information on the variable stiffness–based neutral axis shift is provided in the Supplementary Materials (section 7 of Supplementary Text and fig. S18).

Bidirectional interaction with an organism

The illustration of the in vivo experiment in Fig. 5A shows the capability of using the soft gripper to incubate a snail egg with thermal stimulation while detecting mechanical hatching signals and to detect the heart rate of a newly hatched snail (Institutional Animal Care and Use Committee number 2019-0047). The snail egg used in this experiment belongs to the species *Achatina fulica*, whose eggs have low durability and a diameter of 3 mm (Fig. 5B), making them difficult to hold even with tweezers. The developed gripper that made mechanically conformal and soft contact with an actuation temperature (~39°C) lower than the threshold temperature (43°C, to ensure organism survival (*30*)) was suitable for gripping, manipulation, and transfer of thermal energy for the hatching process, occurring for about 1 week (Fig. 5C). Over this period, the gripper transferred thermal energy and maintained the egg at a temperature of about 30°C, the proper temperature for hatching snail eggs (before heating, fig. S19A; during heating, Fig. 5D). The environmental temperature and humidity remained at 20°C and 70 to 90%, respectively. The graph in fig. S19B shows the change in temperature at three different locations (soft gripper, boundary surface, and middle area of the egg) over a period of 6 hours after gripping and thermal stimulation. The organisms in the control group without the gripper and thermal stimulation all died, mostly because of the low environmental temperature (fig. S19C). The hatching signals, which correspond to a motile stage, were also successfully monitored through the strain sensor despite the relatively low mass of the egg (0.04 g) and slow movement detected by the crack-based strain sensor (Fig. 5E and movie S3). The soft gripper further measured the heart rate of the newly hatched snail, as shown in Fig. 5F. Here, a micrographic examination of the heart size verified that the heart was beating (Fig. 5G). The soft gripper in conformal contact with the newly hatched snail monitored the heart rate and detected the heartbeat every 0.9 s (1.12 Hz) (Fig. 5H and movie S4). For comparison, the gripper was used to monitor the heart rate of a grown juvenile snail 4 weeks after hatching. The measured rate was 0.64 and 0.9 Hz at 18° and 28°C, respectively, slower than that of the newly hatched snail (fig. S21). This result confirms the well-known fact that the heart rate is slower at lower temperatures and as the snail grows (*31*–*33*). A detailed description of this experiment is given in sections 8 and 9 of Supplementary Text.

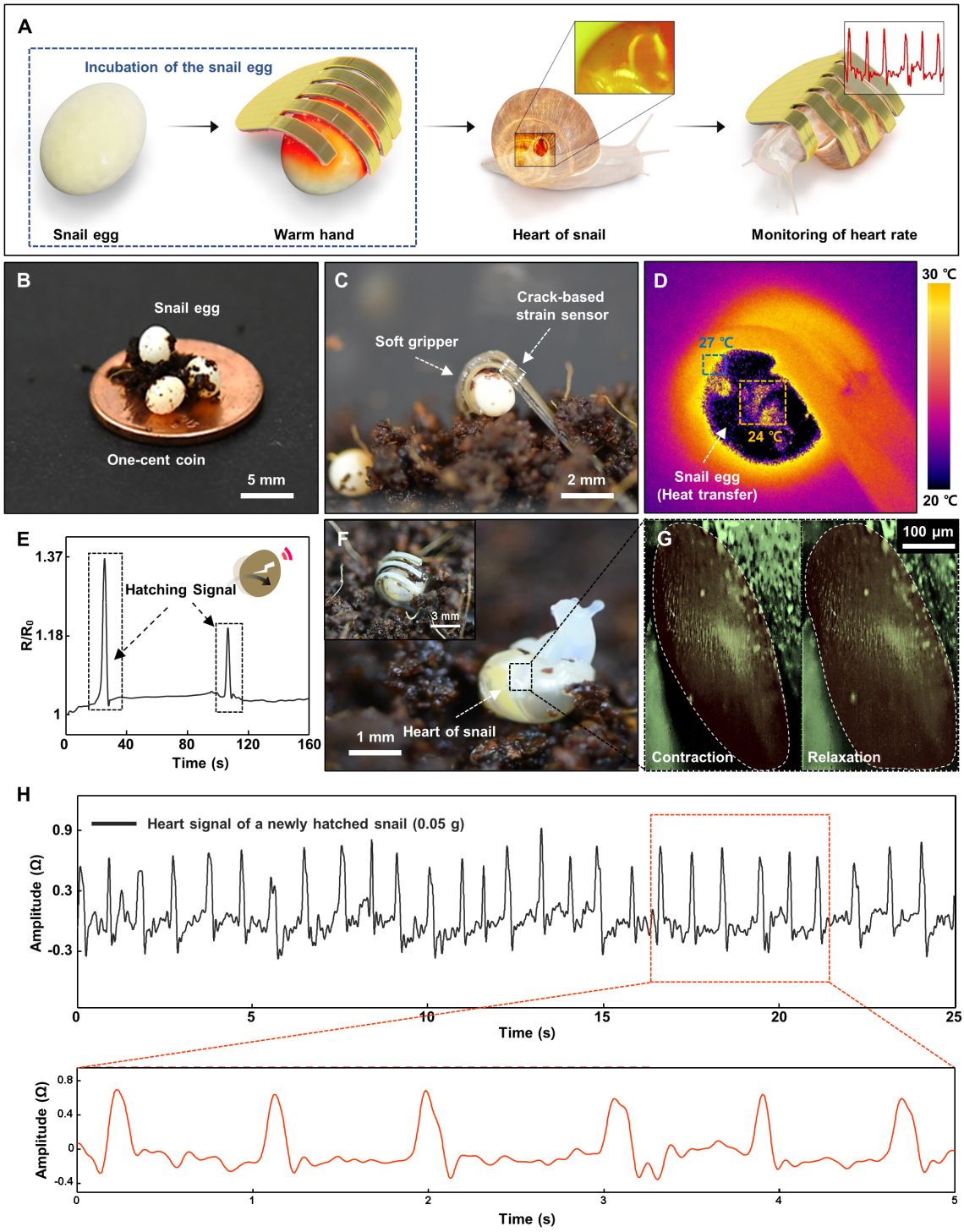

Fig. 5. In vivo experiment to stimulate and monitor the incubation process of a snail from hatching to infancy. (**A**) Illustration of the in vivo experiment with a snail egg and a newly hatched snail. (**B**) Size comparison between the snail egg (~3 mm) and a 1-cent coin (19 mm). (**C**) Soft gripper gripping a snail egg (44 mg) shortly before hatching. (**D**) IR camera image of the snail egg when supplied with heat via the soft gripper. (**E**) Monitoring of the hatching signal originating from snail egg movements. (**F**) Photograph of the newly hatched snail held via the soft gripper (insert image) to measure its heart rate. (**G**) Optical microscope images of the newly hatched snail heart while beating during contraction and relaxation. (**H**) Heart rate of the newly hatched snail extracted from a data acquisition system.

Our experiments with snails demonstrate that the noninvasive hatching process of a small animal through conformal contact with a soft gripper can transfer thermal energy and monitor the physical activity of the animal. Previous devices were able to monitor a heart signal of small size organ or cell, but they could not provide bidirectional interaction for therapy and care (*34*, *35*). All demonstrations and

results in Fig. 5 indicate the potential for replacement of the tools for sensing and stimulation in bio-integrated and implantable electronics with the soft conformal and multifunctional gripper in this article.

CONCLUSION

In this study, we developed and tested a miniaturized multifunctional soft gripper, inspired by the human hand that can interact with organisms. The strengths of our soft gripper include soft and firm gripping of objects using variable stiffness (modulus from 2 MPa to 1.4 GPa) that enables the manipulation of both soft and heavy objects up to a payload capacity of 6400, a bidirectional interaction in which thermal stimulation and simultaneous measurement of biosignals are possible, and miniaturized gripper size for interacting with microscale organisms. We successfully demonstrated the hatching of snail eggs through warm temperature stimulation and monitoring of the heart rate of a newly hatched snail. We believe that our gripper enable the delicate manipulation of complex organisms that require soft conformal mechanics and functional interactions.

To minimize the mechanical mismatch between artificial interfaces and internal organs, recent works in biomedical devices have focused on low stiffness and flexible soft materials (*12*, *36*). In this regard, our soft gripper can be configured for many applications. As a specific example, the gripper could smoothly grip a blood vessel and monitor the blood pressure during cardiovascular surgery without damaging organ tissues. With a proper biocompatible encapsulation layer, this gripper could further enable chronic monitoring of the blood pressure and temperature at various organs (e.g., at a connection between organ blood vessels). In addition, it could enable the triggering of a therapeutic stimulus based on monitored bio-information (*37*). Another potential use is successive fixation of female eggs without damaging the cells during intracytoplasmic sperm injection (ICSI), which is crucial to increase the success rate of ICSI (*38*).

Our current work focuses on scaled in vivo processes involving various organs with bidirectional interactions. The soft gripper that we developed enabled us to document the process of stimulating and monitoring the incubation of snails from hatching to infancy in vivo. Although well configured for various applications, we expect that the following modifications can be made for the further improvement from the current version: manipulation of the finger joint units, fabrication of a multiple sensors for the feedback treatment, and integration with the wireless operation and reversible moving functionalities. The first modification will be made through the laser ablation at joint areas in each finger that would yield pinch gripping of the target object. The consequence is the improved conformal contact with a nondevelopable surface. Integrating multiple and various sensing modalities is another future direction. Here, a daunting challenge is the integration of multiple sensors within a limited area on the gripper. Recent advanced micro- and nanoscale fabrication is the key for the sensor integration and, consequently, the mapping of various signals from gripped object. Wireless operation and reversible moving functionality is necessary for the reusability and convenient operation. We anticipate that the wireless operation will allow for the potential use of the soft gripper as the implantable robotics in the human body. The future soft gripper with all adjustments above would extend the applications in biomedical engineering, such as an implantable, closed-loop operating system applicable to the human body.

MATERIALS AND METHODS

Synthesis of AG NWs

Ag NWs were synthesized by a one-pot polyol method. In this process, polyvinylpyrrolidone (0.32 g; #PVP40, Sigma-Aldrich) and silver nitrate ($AgNO_3$; 0.19 g; #10220, Sigma-Aldrich) were sequentially added to ethylene glycol (EG; 50 ml; #324558, Sigma-Aldrich) and dissolved using a magnetic stirrer bar at 700 rpm for 15 min at room temperature. Then, a solution of ferric chloride ($FeCl_3$; 0.012 M in EG; #451649, Sigma-Aldrich) in EG (0.012 M) was added, and the mixture was thoroughly stirred. The well-dispersed mixture was then placed for 8 hours in a Teflon-lined autoclave reactor preheated to 150°C. Once the NW growth was finished, the reactor was allowed to cool to room temperature. The product was washed using acetone and ethanol and subjected to centrifugation at 4000 rpm for 5 min to remove excess solvent and reagents. The obtained Ag NWs, 70 nm in diameter and 100 to 200 μm in length (aspect ratio, ~2800), were stored in ethanol.

Fabrication of the crack-based strain sensor

The substrate used to fabricate the crack-based strain sensor was a 7.5-μm-thick PI film (3022-5 Kapton thin film, Chemplex, Palm City, FL, USA). A thermal evaporation system (Thermal Evaporation System, DD High Tech. Co., Gimpo-si, South Korea) was used to sequentially deposit a 60-nm-thick layer of chromium as a crack-generating layer and a 20-nm-thick gold layer as an electrical conductor onto the PI film. Cracks were generated by stretching the metal-deposited PI film by 1% at a rate of 10 mm/min using a material testing machine (3342 UTM, Instron Co., Norwood, MA, USA). This process was repeated for about 3000 cycles until the change in the resistance of the sensor converged.

Preparation of the soft gripper

The pellet-type SMP (MM-3520, SMP Technologies Inc., Tokyo, Japan) was processed in film form using a heat press machine (K-223, Lab Tech Science, Daejeon, South Korea). For this procedure, SMP pellets (3.4 g) were sandwiched between Teflon films (FEPO125, Alphaflon, Seoul, South Korea), and aluminum foils and were heat pressed at 160°C and 12 MPa. The fabricated SMP film (thickness of 100 to 400 μm) was cut into 5 cm–by–5 cm strips, prestretched to a strain of 50 to 200% at 70°C for 15 min, and then allowed to cool to ambient temperature. After transfer of the Ag NWs onto the prestretched SMP by a vacuum filtration method, a gel pack (WF-60-X0-A, Hakuto Co., Tokyo, Japan) was attached to the bottom of the prestretched SMP to prevent recovery to the unstretched condition due to the heat generated during ultraviolet (UV) laser processing. The prestretched SMP was cut into the shape of a human hand and patterned using a UV laser ablation method (A series, Oxford Lasers Inc., Shirley, MA, USA). The hand-shaped SMP with laser-patterned Ag NWs was covered with NOA68 (Norland Products Inc., Cranbury, NJ, USA), followed by encapsulation in this noncontracting layer using a UV curing system (MT-UV-O, Minuta Technology, Cheongju-si, South Korea). For measuring an external stimulus, the crack-based strain sensor was incorporated at the bottom of the hand-shaped SMP. More details of the fabrication process are provided in Supplementary Materials and Method.

Calibration and measurement of the temperature sensor

Because the temperature measurements were to be performed on an organism, the following calibration process was performed from 24°

to 40°C on a hot plate. The heat-detecting fingers of the soft gripper were placed on the hot plate, and the temperature sensor was calibrated by gradually increasing the temperature from 24°C in 16 increments of 1°C while using an IR camera (A655SC, FLIR Co., Gangnam-gu, South Korea) to measure the temperature of the fingers. The resistance of the Ag NWs in the fingers gradually increased. These results were used to define the calibration factor for the fingers of the soft gripper so that the soft gripper was able to measure the temperature of an object.

Measurement of biomimetic blood flow

An artificial artery system was designed to evaluate the sensing performance of the soft gripper. The in vitro setup was evaluated by measuring changes in the flow rate through the artificial blood vessel, consisting of a silicone rubber tube (internal diameter of 3.7 mm; thickness of 0.3 to 0.5 mm) with a Young's modulus similar (1.8 MPa) to that of the human carotid artery. Water was pumped through the tube using an adjustable peristaltic pump (KCP PRO-2, Kamoer, Shanghai, China) that operates similarly to a human heart, with the speed of the pump adjusted to control the flow rate between 30 and 260 ml/min.

Characterization of the soft gripper

Field-emission SEM (S-4300SE microscope, Hitachi Ltd., Tokyo, Japan) was used to analyze the cross sections and surfaces of the soft gripper. An IR camera (A655SC, FLIR Co., Gangnam-Gu, South Korea) was used to obtain voltage-temperature data during Ag NW heating. The vertical pulling force and Young's modulus were measured using a universal testing machine (3342 UTM, Instron Co., Norwood, MA, USA). The curvatures of the soft gripper were measured from optical microscope images (U-MSSPQ microscope, Olympus, Tokyo, Japan). A LabVIEW-based data acquisition system (NI PXI-1033, National Instruments Inc., Austin, TX, USA) was used to collect all relevant data. A 4-Fr sheath was inserted into the pig artery as the aortic pressure and wave were recorded with a RadiAnalyzer (Abbott Vascular, Santa Clara, CA, USA).

SUPPLEMENTARY MATERIALS

www.science.org/doi/10.1126/scirobotics.abi6774
Materials and Methods
Text
Figs. S1 to S21
Tables S1 and S2
Movies S1 to S4
References (*39*–*46*)

REFERENCES AND NOTES

1. H. Shen, Meet the soft, cuddly robots of the future. *Nature* **530**, 24–26 (2016).
2. D. Rus, M. T. Tolley, Design, fabrication and control of soft robots. *Nature* **521**, 467–475 (2015).
3. J. Langowski, P. Sharma, A. L. Shoushtari, In the soft grip of nature. *Sci. Robot.* **5**, eabd9120 (2020).
4. S. Terryn, J. Brancart, D. Lefeber, G. Van Assche, B. Vanderborght, Self-healing soft pneumatic robots. *Sci. Roboti.* **2**, eaan4268 (2017).
5. A. K. Mishra, T. J. Wallin, W. Pan, P. Xu, K. Wang, E. P. Giannelis, B. Mazzolai, R. F. Shepherd, Autonomic perspiration in 3D-printed hydrogel actuators. *Sci. Robot.* **5**, eaaz3918 (2020).
6. J. Kim, M. Lee, H. J. Shim, R. Ghaffari, H. R. Cho, D. Son, Y. H. Jung, M. Soh, C. Choi, S. Jung, K. Chu, D. Jeon, S.-T. Lee, J. H. Kim, S. H. Choi, T. Hyeon, D.-H. Kim, Stretchable silicon nanoribbon electronics for skin prosthesis. *Nat. Commun.* **5**, 5747 (2014).
7. C. Majidi, Soft sensors that can feel it all. *Sci. Robot.* **5**, eabf0894 (2020).
8. S. I. Rich, R. J. Wood, C. Majidi, Untethered soft robotics. *Nat. Electron.* **1**, 102–112 (2018).
9. A. Ghosh, L. Li, L. Xu, R. P. Dash, N. Gupta, J. Lam, Q. Jin, V. Akshintala, G. Pahapale, W. Liu, A. Sarkar, R. Rais, D. H. Gracias, F. M. Selaru, Gastrointestinal-resident, shape-changing microdevices extend drug release in vivo. *Sci. Adv.* **6**, eabb4133 (2020).
10. M. Sitti, Miniature soft robots—Road to the clinic. *Nat. Rev. Mater.* **3**, 74–75 (2018).
11. R. L. Truby, M. Wehner, A. K. Grosskopf, D. M. Vogt, S. G. M. Uzel, R. J. Wood, J. A. Lewis, Soft somatosensitive actuators via embedded 3D printing. *Adv. Mater.* **30**, 1706383 (2018).
12. M. Cianchetti, C. Laschi, A. Menciassi, P. Dario, Biomedical applications of soft robotics. *Nat. Rev. Mater.* **3**, 143–153 (2018).
13. K. B. Justus, T. Hellebrekers, D. D. Lewis, A. Wood, C. Ingham, C. Majidi, P. R. LeDuc, C. Tan, A biosensing soft robot: Autonomous parsing of chemical signals through integrated organic and inorganic interfaces. *Sci. Robot.* **4**, eaax0765 (2019).
14. B. Shih, D. Shah, J. Li, T. G. Thuruthel, Y. L. Park, F. Iida, Z. Bao, R. Kramer-Bottiglio, M. T. Tolley, Electronic skins and machine learning for intelligent soft robots. *Sci. Robot.* **5**, eaaz9239 (2020).
15. H. Imamura, K. Kadooka, M. Taya, A variable stiffness dielectric elastomer actuator based on electrostatic chucking. *Soft Matter* **13**, 3440–3448 (2017).
16. J. Shintake, B. Schubert, S. Rosset, H. Shea, D. Floreano, Variable stiffness actuator for soft robotics using dielectric elastomer and low-melting-point alloy, in *2015 IEEE/RSJ International Conference on Intelligent Robots and Systems (IROS)* (IEEE, 2015), pp. 1097–1102.
17. W. Wang, C. Li, M. Cho, S.-H. Ahn, Soft tendril-inspired grippers: Shape morphing of programmable polymer–paper bilayer composites. *ACS Appl. Mater. Interfaces* **10**, 10419–10427 (2018).
18. W. Wang, S.-H. Ahn, Shape memory alloy-based soft gripper with variable stiffness for compliant and effective grasping. *Soft Robot.* **4**, 379–389 (2017).
19. E. Brown, N. Rodenberg, J. Amend, A. Mozeika, E. Steltz, M. R. Zakin, H. Lipson, H. M. Jaeger, Universal robotic gripper based on the jamming of granular material. *Proc. Natl. Acad. Sci. U.S.A.* **107**, 18809–18814 (2010).
20. Z. Xie, A. G. Domel, N. An, C. Green, Z. Gong, T. Wang, E. M. Knubben, J. C. Weaver, K. Bertoldi, L. Wen, Octopus arm-inspired tapered soft actuators with suckers for improved grasping. *Soft Robot.* **7**, 639–648 (2020).
21. D. Kang, P. V. Pikhitsa, Y. W. Choi, C. Lee, S. S. Shin, L. Piao, B. Park, K. Y. Suh, T. I. Kim, M. Choi, Ultrasensitive mechanical crack-based sensor inspired by the spider sensory system. *Nature* **516**, 222–226 (2014).
22. S. M. Mirvakili, I. W. Hunter, Artificial muscles: Mechanisms, applications, and challenges. *Adv. Mater.* **30**, 1704407 (2018).
23. A. Cho, Pretty as you please, curling films turn themselves into nanodevices. *Science* **313**, 164–165 (2006).
24. S. Janbaz, R. Hedayati, A. Zadpoor, Programming the shape-shifting of flat soft matter: From self-rolling/self-twisting materials to self-folding origami. *Mater. Horiz.* **3**, 536–547 (2016).
25. P. S. Yarmolenko, E. J. Moon, C. Landon, A. Manzoor, D. W. Hochman, B. L. Viglianti, M. W. Dewhirst, Thresholds for thermal damage to normal tissues: An update. *Int. J. Hyperthermia* **27**, 320–343 (2011).
26. W. A. D. M. Jayathilaka, K. Qi, Y. Qin, A. Chinnappan, W. Serrano-García, C. Baskar, H. Wang, J. He, S. Cui, S. W. Thomas, S. Ramakrishna, Significance of nanomaterials in wearables: A review on wearable actuators and sensors. *Adv. Mater.* **31**, 1805921 (2019).
27. W. A. Riley, R. W. Barnes, G. W. Evans, G. L. Burke, Ultrasonic measurement of the elastic modulus of the common carotid artery. The Atherosclerosis Risk in Communities (ARIC) Study. *Stroke* **23**, 952–956 (1992).
28. G. Lee, Y. W. Choi, T. Lee, K. S. Lim, J. Shin, T. Kim, H. K. Kim, B.-K. Koo, H. B. Kim, J.-G. Lee, K. Ahn, E. Lee, M. S. Lee, J. Jeon, H. S. Yang, P. Won, S. Mo, N. Kim, M. H. Jeong, Y. Roh, S. Han, J.-S. Koh, S. M. Kim, D. Kang, M. Choi, Nature-inspired rollable electronics. *NPG Asia Mater.* **11**, 67 (2019).
29. G. Lee, M. C. Kim, Y. W. Choi, N. Ahn, J. Jang, J. Yoon, S. M. Kim, J. G. Lee, D. Kang, H. S. Jung, M. Choi, Ultra-flexible perovskite solar cells with crumpling durability: Toward a wearable power source. *Energ. Environ. Sci.* **12**, 3182–3191 (2019).
30. S. Sharma, K. Dickens, Effect of temperature and egg laying depths on giant African land snail (Gastropoda: Achatinidae) viability. *Fla. Entomol.* **101**, 150–151 (2018).
31. H. A. Woods, W. Makino, J. B. Cotner, S. E. Hobbie, J. F. Harrison, K. Acharya, J. J. Elser, Temperature and the chemical composition of poikilothermic organisms. *Funct. Ecol.* **17**, 237–245 (2003).
32. L. Renwrantz, F. Spielvogel, Heart rate and hemocyte number as stress indicators in disturbed hibernating vineyard snails, *Helix pomatia*. *Comp. Biochem. Physiol. Part A Mol. Integr. Physiol.* **160**, 467–473 (2011).
33. V. L. Zhuravlev, D. D. Piatsy, E. E. Titarenko, T. A. Safonova, S. V. Shabelnikov, S. A. Kodirov, Comparison of heart rate in embryonic, young and adult *Achatina fulica*. *Molluscan Res.* **37**, 133–139 (2017).
34. D.-S. Kim, Y.-J. Jeong, B.-K. Lee, A. Shanmugasundaram, D.-W. Lee, Piezoresistive sensor-integrated PDMS cantilever: A new class of device for measuring the drug-induced changes in the mechanical activity of cardiomyocytes. *Sens. Actuators B* **240**, 566–572 (2017).

35. F. Santoso, V. V. Krylov, A. L. Castillo, F. Saputra, H. M. Chen, H. T. Lai, C. D. Hsiao, Cardiovascular performance measurement in water fleas by utilizing high-speed videography and imagej software and its application for pesticide toxicity assessment. *Animals* **10**, 1587 (2020).
36. Y. Kim, G. A. Parada, S. Liu, X. Zhao, Ferromagnetic soft continuum robots. *Sci. Robot.* **4**, eaax7329 (2019).
37. C. M. Boutry, L. Beker, Y. Kaizawa, C. Vassos, H. Tran, A. C. Hinckley, R. Pfattner, S. Niu, J. Li, J. Claverie, Z. Wang, J. Chang, P. M. Fox, Z. Bao, Biodegradable and flexible arterial-pulse sensor for the wireless monitoring of blood flow. *Nat. Biomed. Eng.* **3**, 47–57 (2019).
38. F. Sadak, M. Saadat, A. M. Hajiyavand, Three dimensional auto-alignment of the ICSI pipette. *IEEE Access* **7**, 99360–99370 (2019).
39. M. Bodaghi, R. Noroozi, A. Zolfagharian, M. Fotouhi, S. Norouzi, 4D printing self-morphing structures. *Materials* **12**, 1353 (2019).
40. X.-G. Guo, Z.-F. Zhou, C. Sun, W.-H. Li, Q.-A. Huang, A simple extraction method of Young's modulus for multilayer films in MEMS applications. *Micromachines* **8**, 201 (2017).
41. J. Amend, N. Cheng, S. Fakhouri, B. Culley, Soft robotics commercialization: Jamming grippers from research to product. *Soft Robot.* **3**, 213–222 (2016).
42. A. Chortos, Z. Bao, Skin-inspired electronic devices. *Mater. Today* **17**, 321–331 (2014).
43. W. Wu, X. Wen, Z. L. Wang, Taxel-addressable matrix of vertical-nanowire piezotronic transistors for active and adaptive tactile imaging. *Science* **340**, 952–957 (2013).
44. D. M. Drotlef, M. Amjadi, M. Yunusa, M. Sitti, Bioinspired composite microfibers for skin adhesion and signal amplification of wearable sensors. *Adv. Mater.* **29**, 1701353 (2017).
45. Y. Ma, N. Liu, L. Li, X. Hu, Z. Zou, J. Wang, S. Luo, Y. Gao, A highly flexible and sensitive piezoresistive sensor based on MXene with greatly changed interlayer distances. *Nat. Commun.* **8**, 1207 (2017).
46. Y. Wu, Y. Liu, Y. Zhou, Q. Man, C. Hu, W. Asghar, F. Li, Z. Yu, J. Shang, G. Liu, M. Liao, R.-W. Li, A skin-inspired tactile sensor for smart prosthetics. *Sci. Robot.* **3**, eaat0429 (2018).

Acknowledgments: We thank M. Fouad for helping with the English translation. **Funding:** S.H., D. Kang, and J.-S.K. acknowledge financial support from the Ajou University research fund. This work was supported by the National Research Foundation of Korea (NRF) grant funded by the Korean government (MSIT) (2019R1C1C1007629, 2019R1A2C1090056, 2019R1F1A1063066, and 2021M3H4A1A01079367) and the Ministry of Trade, Industry and Energy (MOTIE, Korea) under the Industrial Technology Innovation Program no. 20000512. This work was supported by the Environmental Health Action Program under project 2018001350005 and the Defense Acquisition Program Administration's Critical Technology R&D program (UC190002D). **Author contributions:** Y.R., M.K., S.M.W., J.-S.K., D. Kang, and S.H. were the main contributors to the project. Y.R. and M.K. led the experimental work, with support from D.L., S.L., C.K., D. Kim, D.G., and Seongyeon Kim. manufacturing fabrication of the soft gripper and the crack-based sensors. S.L., D.S., and B.K. performed mechanical modeling. H.K.K. and B.-K.K. performed the in vivo experiments related to implantation surgeries. I.H., T.K., D.L., S.I., and G.L. contributed analysis of the mechanical characterizations for the crack-based sensor. S.W., J.-S.K., D. Kang, and S. H. supervised the work. **Competing interests:** The authors declare that they have no competing interests. **Data and materials availability:** All data needed to evaluate the conclusions in the paper are present in the paper or the Supplementary Materials.

Submitted 24 March 2021
Accepted 20 September 2021
Published 13 October 2021
10.1126/scirobotics.abi6774

Citation: Y. Roh, M. Kim, S. M. Won, D. Lim, I. Hong, S. Lee, T. Kim, C. Kim, D. Lee, S. Im, G. Lee, D. Kim, D. Shin, D. Gong, B. Kim, S. Kim, S. Kim, H. K. Kim, B.-K. Koo, S. Seo, J.-S. Koh, D. Kang, S. Han, Vital signal sensing and manipulation of a microscale organ with a multifunctional soft gripper. *Sci. Robot.* **6**, eabi6774 (2021).

Science Robotics

Vital signal sensing and manipulation of a microscale organ with a multifunctional soft gripper

Yeonwook Roh, Minho Kim, Sang Min Won, Daseul Lim, Insic Hong, Seunggon Lee, Taewi Kim, Changhwan Kim, Doohoe Lee, Sunghoon Im, Gunhee Lee, Dongjin Kim, Dongwook Shin, Dohyeon Gong, Baekgyeom Kim, Seongyeon Kim, Sungyeong Kim, Hyun Kuk Kim, Bon-Kwon Koo, Sungchul Seo, Je-Sung Koh, Daeshik Kang, and Seungyong Han

Sci. Robot. **6** (59), eabi6774. DOI: 10.1126/scirobotics.abi6774

Science Robotics (ISSN 2470-9476) is published by the American Association for the Advancement of Science. 1200 New York Avenue NW, Washington, DC 20005. The title *Science Robotics* is a registered trademark of AAAS.